

Smoothed Rectangular Function-Based FIR Filter Design

Abdelhak Boukharouba¹

Received: 9 April 2016 / Revised: 18 February 2017 / Accepted: 21 February 2017
© Springer Science+Business Media New York 2017

Abstract A new technique for designing FIR filters where the desired frequency response is a smoothed rectangular function is proposed. Instead of choosing a suitable window in time domain, we will directly try smoothing the ideal desired response in frequency domain. The impulse response of the FIR filter is a sampled version of the inverse Fourier transform of the frequency response. In comparison with results reported in the literature, this technique provides the best performance in terms of filter specifications.

Keywords FIR filter · Filter specifications · Gaussian function · Smoothed rectangular function

1 Introduction

Linear digital filters can be classified into two types based on their structures [7, 11]: infinite impulse response (IIR) and finite impulse response (FIR). IIR filters can provide a much better performance than the FIR filters having the same number of coefficients. However, IIR filters do not generally provide linear-phase responses and they may be unstable. Moreover, this filter type may have a multimodal error surface where the design methods are based on a global search procedure [13, 19, 20]. On the other hand, FIR filters are very interesting components in digital signal and image processing applications. For FIR filter design, the main objective is to approximate a desired frequency response using a finite number of FIR filter coefficients. The ideal desired

✉ Abdelhak Boukharouba
boukharouba_abdelhak@hotmail.com

¹ Faculté des Sciences et de la technologie, Département d'Electronique et de Télécommunications, Université 8 Mai 1945 Guelma, BP 401 24000 Guelma, Algeria

frequency response should look like a rectangular function, and the desired specifications in general are: low variation of the ripples in the passband, high attenuation in the stopband and sharp cutoff, which are competing parameters in FIR filter design. Since there is no feedback, they are inherently stable. The popular methods that can be used for designing digital FIR filters are: window method, frequency sampling method and optimization methods. Each method has its own advantages and disadvantages.

Window functions can be divided into two categories; fixed and adjustable window functions. The most used fixed windows are; rectangular, Hanning, Hamming and Blackman windows [5, 18]. On the other hand, the Kaiser window is a kind of adjustable window function [3, 5]. In the frequency sampling method, the discrete Fourier transform (DFT) of the impulse response must correspond exactly to the samples of the desired frequency response. A novel filter design based on convolution window spectrum interpolation is recently proposed [4], which is derived from the classical frequency sampling method. Classical optimization methods (such as weighting least square sense [21] and Parks–McClellan method [10]) are also used for designing digital FIR filters. To improve the performance of the classical methods, many researchers have utilized heuristic evolutionary optimization algorithms such as genetic algorithm (GA), differential evolution (DE), swarm optimization (SO) [1, 2, 6, 8, 15–17, 22].

FIR filter design using the window method exhibits oscillatory behavior around the discontinuity of the ideal frequency response and does not control the passband and stopband ripples. Even if we increase the number of coefficients in the FIR filter approximation, these ripples concentrate near the passband edge frequency and cannot be eliminated. To reduce this effect, we propose a novel solution in the frequency domain. In order to reduce the Gibbs phenomenon, we try smoothing the ideal response frequency to remove the discontinuities at abrupt transitions of the rectangular window by choosing a Gaussian function as a smoother filter response. The impulse response is obtained by applying inverse Fourier transform to the smoothed frequency response, and then the digital version of this response must be truncated and shifted to be causal. After this, a DFT is used to generate the frequency response of the FIR filter.

In the next section, we present a theoretical analysis of the continuous frequency response and the parameters influencing its shape. Next a digital version of this filter is studied to design an improved digital FIR filter.

2 Frequency Response of the Continuous-Time Filter

An important specification is the required frequency response, which is in the shape of a rectangle. Our idea is inspired from the work presented in [12] where a flat-top filter shape produced by the WaveShaper family of programmable optical filters is presented. A desired filter of bandwidth B should look like a rectangular function, from $-B/2$ to $B/2$. In order to design this filter type, we propose to smooth the ideal response frequency to remove the discontinuities at abrupt transitions of the rectangular window. We choose a Gaussian function as a smoother filter response in the frequency domain. Consequently, the desired frequency response is given by the following convolution:

$$D(f) = R(f) * G(f) \quad (1)$$

where the rectangular function is defined by:

$$R(f) = \begin{cases} 1, & \text{if } \frac{-B}{2} \leq f \leq \frac{B}{2} \\ 0, & \text{otherwise} \end{cases} \quad (2)$$

and the Gaussian function is defined by the following expression:

$$G(f) = \frac{1}{\sigma\sqrt{2\pi}} \exp\left(-\frac{f^2}{2\sigma^2}\right) \quad (3)$$

The analytical expression of the frequency response for continuous-time filter can be expressed as:

$$D_c(f) = \frac{1}{2} \left[\operatorname{erf}\left(\frac{B/2 - f}{\sqrt{2}\sigma}\right) - \operatorname{erf}\left(\frac{-B/2 - f}{\sqrt{2}\sigma}\right) \right] \quad (4)$$

where $\operatorname{erf}(\cdot)$ is the error function defined as follow:

$$\operatorname{erf}(x) = \frac{2}{\sqrt{\pi}} \int_0^x \exp(-t^2) dt \quad (5)$$

This frequency response has two independent parameters, namely the bandwidth of the rectangular function (B) and the adjustable shape parameter (σ), which is the standard deviation of the Gaussian function. The standard deviation (σ) has a constant value in [12] because it characterizes a physical (optical) channel. However, in this work, this parameter is variable and plays a major role to adjust the filter specifications.

To study the effect of the parameter σ on the filter specifications, we compute and plot the frequency response for the continuous-time filter with fixed bandwidth B and different values of σ . By adjusting the parameter σ , the resulting frequency response can closely approximate the desired response. Figure 1 shows the frequency response of the continuous-time filter with fixed bandwidth $B = 4$ and different values of σ . We can notice that the effect of convolution with a Gaussian is to smooth out the sharp transitions of the rectangular function according to the standard deviation value (σ). For larger values of σ , the frequency response becomes narrower at the top and wider at the bottom, whereas for small values of σ the frequency response becomes very close to the ideal response.

Once the desired frequency response has been obtained, the analytical expression of the impulse response is calculated using inverse Fourier transform.

$$d_c(t) = B \operatorname{sinc}(Bt) \exp(-2\pi^2\sigma^2t^2) \quad (6)$$

Figure 2 shows the sinc function with $B = 4$, Gaussian function with $\sigma = 0.5$ and the resultant impulse response which is defined as the multiplication of the Gaussian and the sinc function. As we know, the effective width of the desired impulse response

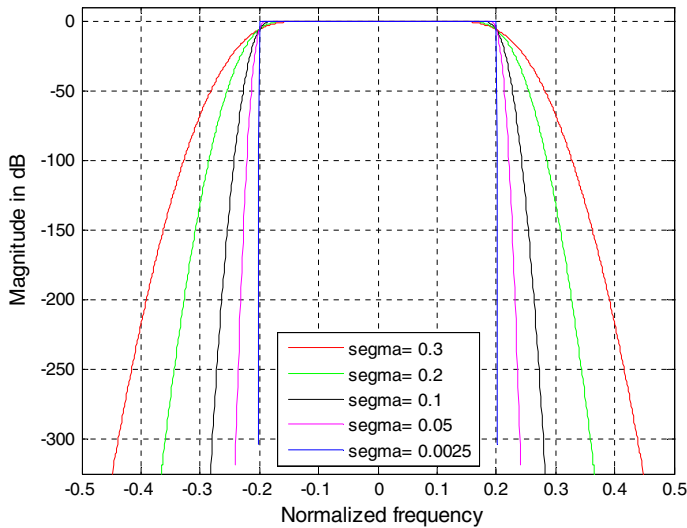


Fig. 1 Frequency response of the continuous-time filter with fixed bandwidth $B = 4$ and different values of σ

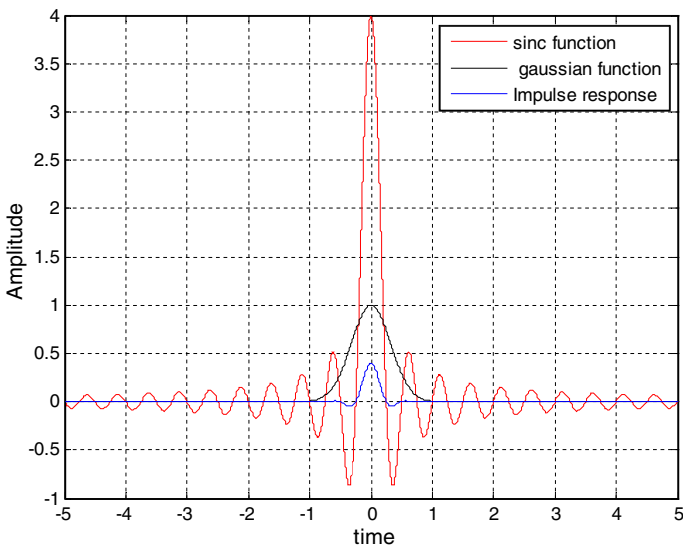


Fig. 2 Impulse response of the continuous filter with $B = 4$ and $\sigma = 0.5$

should be as small as possible. From Fig. 2, we notice that the impulse response of the filter is a narrow function where the two functions have a mutual contribution. The Gaussian function reduces the side lobes of the sinc function, whereas the latter narrows the width of the Gaussian function. Consequently, the impulse response can satisfy significantly the requirements of a desired filter in the time domain.

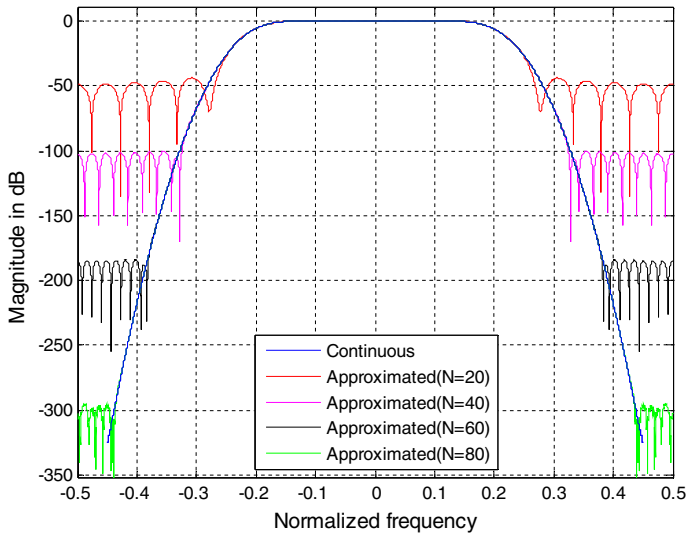


Fig. 3 Frequency response of the FIR filter for $B = 4$, $\sigma = 0.3$ and different values of N

3 Digital FIR Filter Design Approach

As illustrated in Fig. 1, the resulting filter is approximately band-limited. Consequently, the impulse response can be sampled with sampling frequency f_s greater than twice the maximum frequency of the analog spectrum. To obtain the discrete-time filter's impulse response $d(n)$, the continuous-time filter's impulse response $d_c(t)$ is sampled with sampling period $T_s = 1/f_s$.

$$d(n) = T_s d_c(nT_s) \quad (7)$$

The impulse response is sampled with $T_s = 0.1$ second, which verifies the Shannon's sampling theorem. These samples are infinite in length and can be truncated and delayed to get realizable FIR filter for implementation. The impulse response converges rapidly toward zero as shown in Fig. 2, and therefore it is appropriate to reduce the number of coefficients by removing those which are sufficiently close to zero.

The frequency response of this FIR filter has three independent parameters: the bandwidth of the rectangular function B , the adjustable parameter σ and the filter order N . For desired value of B , both parameters σ and N can be adjusted to satisfy the requirements of a desired filter in frequency domain. To study the effect of the filter order N on the FIR filter specifications, we plot the frequency response for fixed values of B and σ and with different values of N and compare them with the frequency response of the continuous-time filter as shown in Fig. 3. This filter has no noticeable ripples in the passband and preserves practically the shape of the frequency response of the continuous filter according to the filter order N . We can also see that the larger N is, the better the frequency response of the FIR filter. However, in this case, the frequency response does not have a rapid roll-off in the transition band. As shown

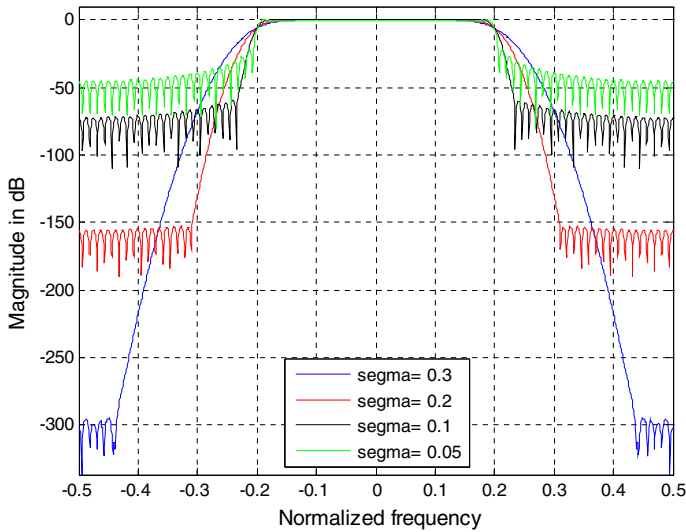


Fig. 4 Frequency response of the FIR filter with fixed bandwidth $B = 4$, $N = 80$ and different values of σ

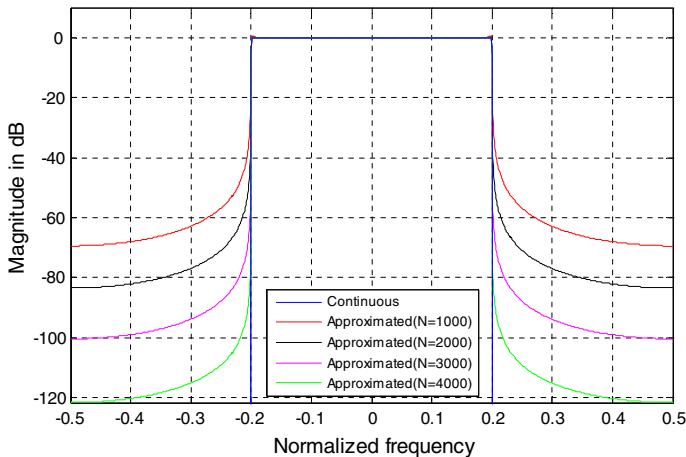


Fig. 5 Frequency response for $B = 4$, $\sigma = 0.0025$ and different values of N

in Fig. 1, to reduce the transition band, we must diminish the value of σ . Figure 4 shows the frequency response of the FIR filter with $B = 4$, $N = 80$ and different values of σ . For fixed N , we can notice that the transition width is reduced when σ diminishes, whereas the stop band attenuation is diminished. Figure 5 shows the frequency response of the resulting filter with $B = 4$, $\sigma = 0.0025$ and different values of N where the frequency response decreases rapidly and does not have any sidelobe. To increase the stop band attenuation, we must then increase the filter order N . Consequently, the stop band attenuation increases at the expense of a larger filter order.

Table 1 Comparison with some recent reported results

Approach	Filter order	Maximum stopband attenuation (dB)	Transition width
[1]	30	<30	0.1
[3]	50	48.98	–
[4]	30	44.45	0.1712
[4]	198	44.12	0.0267
[6]	20	<27	>0.13
[8]	33	<29	–
[15]	30	38.96	0.1712
[16]	20	33.99	0.0946
[21]	198	43.19	0.0267
[22]	20	33.01	0.1203
Our algorithm			
($\sigma = 0.0225$)	20	33.43	0.1720
($\sigma = 0.0195$)	30	45.50	0.1750
($\sigma = 0.0031$)	198	44.52	0.0267

4 Results Analysis and Discussions

To evaluate the performance of FIR LP filter using a smoothed rectangular function, we compare it with other reported results using a sampling frequency $f_s = 1$ Hz. First, the comparison is performed against an improved adjustable window-based technique and a method based on frequency sampling. Afterward, the comparison is done with more sophisticated algorithms based on meta-heuristic optimization. Table 1 summarizes the comparison with some excellent and recent reported results in terms of the filter order N , stop band attenuation and transition width.

For window method, some improved results are reported in [3] where a comparison between different windows is carried out. The first row of the Table 1 shows the best results in terms of maximum stop band attenuation (48.98 dB) for a filter order equal to 50. Some results of frequency sampling method based on convolution window spectrum interpolation are reported in the second and third row [4], whereas the fourth row shows the best results using eigenfilter design method [21]. The next six rows show some recent results using meta-heuristic optimization methods in terms of stop band attenuation and transition width. The best results are reported in [16] for 20th order LP filter where the maximum stopband attenuation achieved is 33.99 dB and the transition width is equal to 0.0946. Figure 6 illustrates a comparison of frequency response based on smoothed rectangular function (SRF) with the ADEPSO algorithm [22] and CSO algorithm [16]. It is also observed that the ADEPSO algorithm achieves practically the same results as compared to those of CSO algorithm because the transition width is calculated from the last passage through 0 dB in the former while it is calculated from the passband edge frequency that is determined by the peak ripple in the passband in the latter. For the same order $N = 20$, our algorithm achieves practically the same maximum stop band attenuation (33.43 dB) as ADEPSO [22] and CSO [16]

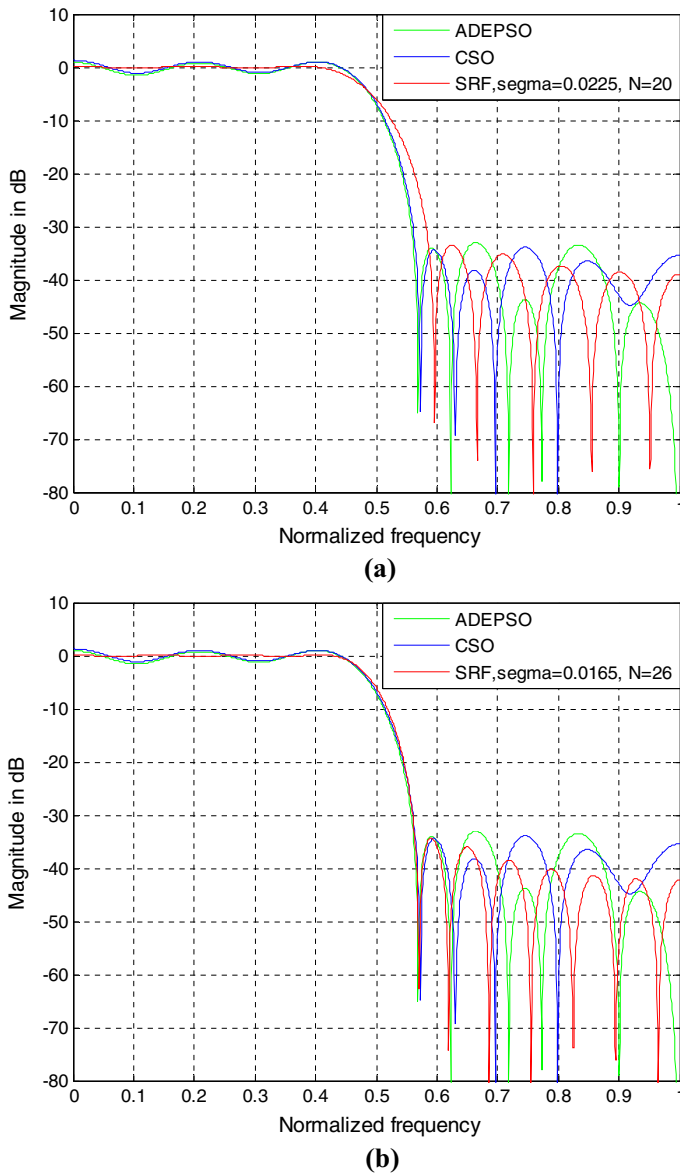


Fig. 6 Comparison with ADEPSO and CSO algorithm **a** Frequency response for $N = 20$ and $\sigma = 0.0225$, **b** Frequency response for $N = 26$ and $\sigma = 0.0165$

algorithms but with larger transition width as shown in Table 1. Compared to these two algorithms, our filter has no noticeable ripples in the passband, whereas the maximum passband ripple is approximately 1.53 dB using CSO algorithm where the transition bandwidth is reduced because of the passband ripples, despite their existence is a major inconvenient for the filter design. If we use the same maximum passband ripple

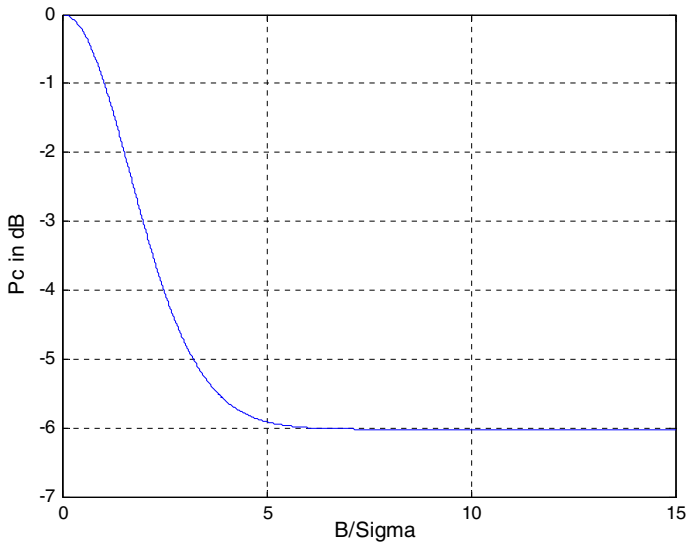


Fig. 7 Magnitude of P_c in dB

to calculate the transition width in our algorithm, the transition width is reduced to 0.136. As conclusion, the reduced transition width in the reported results is achieved at expense of the passband ripples.

Consequently, the SRF-based filter has a maximally flat response without passband ripple and high stopband attenuation at the cost of a relatively wide transition region. We have also used the mean squared error (MSE) between the resulting frequency response and the desired one (rectangular function) to compare the global approximation error. The magnitude response is compared against 1 for the range of frequencies less than or equal to the cutoff frequency f_c and against 0 otherwise where f_c is equal to 0.5 in this comparison and the mean square error (MSE) is calculated by taking the average of the instantaneous error using the following formula.

$$\text{MSE} = \frac{1}{L} \sum_{k=0}^{L-1} e_k^2 \quad (8)$$

where L is the length of the frequency response. As a result, the error is 0.0126 and 0.0124 for the results in [22] and [16] respectively. However, the error in our work is 0.0121 and, consequently, the proposed algorithm is the best in the mean squared error sense. Moreover, from Fig. 6a, it is also the best in the minimax sense, which minimizes the maximum of the absolute error between the resulting frequency response and the ideal response in the passband and stopband regions. To reduce the transition width and increase the stop band attenuation, we must diminish the value of σ and increase the filter order N as shown in Fig. 6b where for $N = 26$, we can ensure the same results as ADEPSO and CSO algorithms in terms of maximum stop band attenuation and transition width with no noticeable ripple in the passband region.

In the case of high-order FIR filters ($N = 198$), the algorithm is compared with two approaches [4, 21] as shown in Table 1. We can observe that for the same achieved transition width 0.0267, the maximum stop band attenuation is 44.12 dB in [4] and 43.19 dB in [21], whereas in our approach is 44.52 dB. Consequently, for the same filter order and transition width, the performance of the proposed algorithm is slightly better in terms of maximum stop band attenuation. As explained in [4], most of classical optimization methods do well in providing an excellent transfer characteristic. However, they are realized by multiple iterations of updating parameters until convergence. In addition, evolutionary optimization methods are also not competent in designing high-order FIR filters due to their heavy computation and unguaranteed convergence. Hence, these algorithms are not suitable for designing high-order linear-phase FIR filters. On the other hand, the proposed algorithm do well in designing high-order FIR filters using a simple sampling of the impulse response. Moreover, we can design FIR filters with sharp transition band and without any ripples in the passband region as shown in Fig. 5 but at the expense of a larger filter order.

Another advantage of this algorithm is the stability of the -6.02 dB cutoff frequency which is nearly located at $B/2$. As the desired frequency response is a rectangular function with bandwidth B , the desired cutoff frequency is $B/2$ which is identified as the point where the resulting filter shape crosses the ideal rectangular window. This level is given in [12].

$$Pc = \frac{1}{2} \operatorname{erfc}\left(\frac{B}{\sqrt{2}\sigma}\right) / \operatorname{erfc}\left(\frac{B}{2\sqrt{2}\sigma}\right) \quad (9)$$

We can verify that Pc tends to $1/2$ as B/σ increases. Figure 7 illustrates the magnitude of Pc in dB where the -6 dB cutoff frequency point is achieved when B/σ equal to 6.08, and for all values of B/σ greater than 7.9, the -6.02 dB cutoff frequency will be stabilized at $B/2$. As discussed above, the standard deviation must be much smaller than the filter bandwidth to ensure a best approximation. For all above cases, the crossover point is located at $B/2$ and -6.02 dB and consequently, the proposed algorithm has a high robustness in controlling the -6 dB cutoff frequency point. Compared to reported results, the proposed algorithm provides the best performance in terms of filter specifications where the best solution can be chosen as the trade-off between the transition width and the maximum stop band attenuation.

We can also directly design a linear-phase bandpass filter from a designed lowpass filter by modulation, $d_{bp}(kT_e) = 2d(kT_e) \cos(2\pi f_0 kT_e)$ [9, 14]. The bandpass FIR filter is a shifted and truncated version of the d_{bp} . This filter has also a linear-phase transfer function of the same type and the same order as the lowpass filter.

This algorithm is the most straightforward among the other reported techniques, and it is the better in terms of both time complexity and optimal performance for filter design. Moreover, meta-heuristic optimization methods use objective functions which are multimodal in nature and highly nonlinear in the most cases. They are extremely sensitive to starting points, and they may easily be trapped in local minima. To converge surly to the global minimum, the algorithm must be run many times, for example, in [16] each algorithm is run for 50 times to obtain its best results. Consequently, they are very expensive in terms of execution time.

5 Conclusion

In this paper, an efficient way of designing linear-phase FIR filters using a smoothed rectangular function as a frequency response is presented. The smoothed rectangular function should be as close as possible to the ideal frequency response. In the proposed approach, we have made an analytical study in the frequency domain and once the desired frequency response is obtained, the impulse response is calculated directly as inverse Fourier transform of the frequency response. The impulse response of the FIR filter is obtained by sampling the continuous impulse response, whereas in the other works that are based on the windowing method, they propose different windows in discrete time and study their effect on the frequency response with any prior idea about the specifications in frequency domain.

The main advantage of this algorithm is its flexibility thanks to the three tunable parameters, which allow a robust adjustment of the compromise between the stop band attenuation and the transition width. Moreover, we can design tunable FIR bandpass filters where for a desired center frequency, an appropriate bandwidth is achieved by tuning these parameters according to the application requirements. Consequently, this simple algorithm can be used to design reconfigurable filters for many applications in communication systems. On the other hand, the major drawback of optimization algorithms is that they require a high computational cost to achieve the desired specifications. They depend on a lot of parameters, and the choice of them has an important impact on optimization performance. Moreover, the parameter choice and the convergence of these algorithms depend only on empirical results. As conclusion, the proposed algorithm do well in designing FIR filters of any order using a simple sampling of the impulse response.

References

1. J.I. Ababneh, M.H. Bataineh, Linear phase FIR filter design using particle swarm optimization and genetic algorithms. *Digit. Signal Process.* **18**(4), 657–668 (2008)
2. S.U. Ahmad, A. Antoniou, A genetic algorithm approach for fractional delay FIR filters. in *IEEE International Symposium on Circuits and Systems, ISCAS 2006*, pp. 2517–2520
3. K. Avci, A. Nacaroglu, Cosh window family and its application to FIR filter design. *Int. J. Electron. Commun.* **63**, 907–916 (2009)
4. X. Huang, S. Jing, Z. Wang, Y. Xu, Y. Zheng, Closed-form FIR filter design based on convolution window spectrum interpolation. *IEEE Trans. Signal Process.* **64**(5), 1173–1186 (2016)
5. J.F. Kaiser, R.W. Schafer, On the use of the IO-sinh window for spectrum analysis. *IEEE Trans. Acoust. Speech Signal Process* **28**, 105–107 (1980)
6. B. Luitel, G.K. Venayagamoorthy, Differential evolution particle swarm optimization for digital filter design. in *IEEE Congress on Evolutionary Computation, CEC 2008*, pp. 3954–3961
7. S.K. Mitra, J.F. Kaiser, *Handbook for Digital Signal Processing* (Wiley, New York, 1993)
8. M. Najjarzadeh, A. Ayatollahi, FIR digital filters design: particle swarm optimization utilizing LMS and minimax strategies. in *IEEE International Symposium on Signal Processing and Information Technology, 2008*, pp. 129–132
9. Y. Neuvo, G. Rajan, S.K. Mitra, Design of narrow-band FIR bandpass digital filters with reduced arithmetic complexity. *IEEE Trans. Circuits Syst.* **34**(4), 409–419 (1987)
10. T. Parks, J. McClellan, Chebyshev approximation for nonrecursive digital filters with linear phase. *IEEE Trans. Circuits Theory* **19**(2), 189–194 (1972)
11. W. Parks, C.S. Burrus, *Digital Filter Design* (Wiley, New York, 1987)

12. C. Pulikkaseril, Filter Bandwidth Definition of the WaveShaper S-series Programmable Processor, Finisar product whitepaper
13. M. Radenkovic, T. Bose, Adaptive IIR filtering of nonstationary signals. *Sig. Process.* **81**, 183–195 (2001)
14. G. Rajan, Y. Neuvo, S.K. Mitra, On the design of sharp cutoff wide-band FIR filters with reduced arithmetic complexity. *IEEE Trans. Circuits Syst.* **35**(11), 1447–1454 (1988)
15. K.S. Reddy, S.K. Sahoo, An approach for FIR filter coefficient optimization using differential evolution algorithm. *AEU-Int. J. Electron. Commun.* **69**(1), 101–108 (2015)
16. S.K. Saha, S.P. Ghoshal, R. Kar, D. Mandal, Cat Swarm Optimization algorithm for optimal linear phase FIR filter design. *ISA Trans.* **52**(6), 781–794 (2013)
17. S. Salcedo-Sanz, F. Cruz-Roldan, C. Heneghan, X. Yao, Evolutionary design of digital filters with application to subband coding and data transmission. *IEEE Trans. Signal Process.* **55**(4), 1193–1203 (2007)
18. T. Saramaki, A class of window functions with nearly minimum sidelobe energy for designing fir filters. in *Proceedings of the IEEE International Symposium Circuits and Systems, Portland, USA*, pp. 359–362 (1989)
19. J.J. Shynk, Adaptive IIR filtering. *IEEE ASSP Mag.* **6**, 4–21 (1989)
20. S.D. Stearns, Error surface of recursive adaptive filters. *IEEE Trans. Acoust. Speech Signal Process.* **29**, 763–766 (1981)
21. P. Vaidyanathan, T. Nguyen, Eigenfilters: a new approach to least-squares FIR filter design and applications including Nyquist filters. *IEEE Trans. Circuits Syst.* **34**(1), 11–23 (1987)
22. Vasundhara, D. Mandal, R. Kar, S.P. Ghoshal, Digital FIR filter design using fitness based hybrid adaptive differential evolution with particle swarm optimization. *Nat. Comput.* **13**(1), 55–64 (2014)